Added value of high resolution models in simulating global precipitation characteristics

ATMOSPHERIC SCIENCE LETTERS
Atmos. Sci. Let. **17**: 646–657 (2016)
Published online in Wiley Online Library
(wileyonlinelibrary.com) **DOI:** 10.1002/asl.715

RMetS
Royal Meteorological Society

Added value of high resolution models in simulating global precipitation characteristics

Lixia Zhang,[1,2,*] Peili Wu,[3] Tianjun Zhou,[1] Malcolm J. Roberts[3] and Reinhard Schiemann[4]

[1]*LASG, Institute of Atmospheric Physics, Chinese Academy of Sciences, Beijing, China*
[2]*Collaborative Innovation Center on Forecast and Evaluation of Meteorological Disasters, Nanjing University of Information Science and Technology, China*
[3]*Met Office Hadley Centre, Exeter, UK*
[4]*Department of Meteorology, Reading University, UK*

**Correspondence to:*
L. Zhang, LASG, Institute of Atmospheric Physics, Chinese Academy of Sciences, Beijing 100029, China.
E-mail: lixiazhang@mail.iap.ac.cn

Received: 16 May 2016
Revised: 25 October 2016
Accepted: 26 October 2016

Abstract

Climate models tend to overestimate percentage of the contribution (to total precipitation) and frequency of light rainfall while underestimate the heavy rainfall. This article investigates the added value of high resolution of atmospheric general circulation models (AGCMs) in simulating the characteristics of global precipitation, in particular extremes. Three AGCMs, global high resolution atmospheric model from the Geophysical Fluid Dynamics Laboratory (GFDL-HiRAM), the Meteorological Research Institute-atmospheric general circulation model (MRI-AGCM) and the Met Office Unified Model (MetUM), each with one high and one low resolution configurations for the period 1998–2008 are used in this study. Some consistent improvements are found across all three AGCMs with increasing model resolution from 50–83 to 20–35 km. A reduction in global mean frequency and amount percentile of light rainfall (<11 mm day^{-1}) and an increase of medium to heavy rainfall (>20 mm day^{-1}) are shown in high resolution models of GFDL-HiRAM and MRI-AGCM, while the improvement in MetUM is not obvious. A consistent response to high resolution across the three AGCMs is seen from the increase of light rainfall frequency and amount percentile over the desert regions, particularly over the ocean desert regions. It suppresses the overestimation of CDD over ocean desert regions and makes a better performance in high resolution models of GFDL-HiRAM and MRI-AGCM, but worse in MetUM-N512. The impact of model resolution differs greatly among the three AGCMs in simulating the fraction of total precipitation exceeding the 95th percentile daily wet day precipitation. Inconsistencies among models with increased resolution mainly appear over the tropical oceans and in simulating extreme wet conditions, probably due to different reactions of dynamical and physical processes to the resolution, indicating their crucial role in high resolution modelling.

Keywords: **high resolution modelling; precipitation characteristics; light and heavy rainfall**

1. Introduction

Societal impacts of climate variability and change crucially depend on risks of extreme climate events. Climate models are usually the best tools available for assessing climate risks. Usually contemporary climate models are constrained by computer power to certain limited grid size (model resolution) and level of descriptive details of physical processes (parameterisations), limiting our capability of simulating and predicting climate extremes. Increasing computer powers make it possible for ever higher resolution models to be employed. Precipitation and the hydrological cycle is a key climate process directly linked to droughts and floods affecting the livelihoods of many people. It is also a big challenge to climate modelling community with huge uncertainties in future climate projections. Current climate models all show deficiencies in simulating the observed characteristic distribution of precipitation frequency and intensity, with an over-simulation of rainy days and low daily rainfall amounts but underestimation of heavy precipitation amounts (Dai, 2006; Tu *et al.*, 2009; Kusunoki and Arakawa, 2012). Increasing model resolution has been proposed as an important way to improve model performance and reduce model uncertainties (Palmer, 2014).

Recent studies have demonstrated added values of enhanced resolution of atmospheric general circulation models (AGCMs) in many aspects, including improvements of the large scale atmospheric circulation (Roberts *et al.*, 2009; Shaffrey *et al.*, 2009; Marti *et al.*, 2010; Delworth *et al.*, 2012; Kinter *et al.*, 2013), blocking events (Jung *et al.*, 2012), tropical cyclones (Jung *et al.*, 2006; Manganello *et al.*, 2012) and summer monsoon precipitation (Kitoh and Kusunoki, 2008; Mizuta *et al.*, 2012; Johnson *et al.*, 2015). For example, an analysis on the simulation of two AGCMs of Hadley Centre Global Environment Model (HadGEM) showed that the horizontal resolution could affect the hydrological cycle by increasing (decreasing) precipitation over

Table 1. Information about the three models used in this study.

Model centre	Name	Horizontal resolution	Simulating time	Forcing SST	Reference
MetUM	MetUM-N216	0.83° × 0.55° ~83 × 55 km	1998–2008	OSTIA (Donlon *et al.*, 2012)	Mizielinski *et al.* (2014)
	MetUM-N512	0.35° × 0.23° ~35 × 35 km	1998–2008		
GFDL	GFDL-HiRAM-C180	0.625° × 0.5° ~63 × 50 km	1998–2008	HadISST (Rayner *et al.*, 2003)	Zhao *et al.* (2009)
	GFDL-HiRAM-C360	0.31° × 0.25° ~31 × 25 km	1998–2008		
MRI	MRI-AGCM-2H	0.56° × 0.56° ~56 × 56 km	1998–2008	HadISST	Mizuta *et al.* (2012)
	MRI-AGCM-2S	0.18° × 0.18° ~18 × 18 km	1998–2008		

land (ocean), which makes high resolution simulations closer to observation over the ocean but further away over land (Demory *et al.*, 2014). When increasing the resolution of NCAR CAM5 from T42 to T266, the spatial pattern of annual mean precipitation amount improves significantly and the rainfall over and around the Tibetan Plateau becomes more realistic (Li *et al.*, 2015; Yu *et al.*, 2015). The recent study of Johnson *et al.* (2015) using different resolution configurations of HadGEM1 indicates that improved resolution of the East African Highlands results in the improved representation of the Somali Jet and the finer orography over Indochina and the Maritime Continent can lead to more precipitation over the Maritime Continent islands.

Most of these studies are based on a single model or different versions of the same model. As pointed out by Mizielinski *et al.* (2014), "The role of resolution in different physical processes in the climate system is not necessarily the same". Consistency of resolution sensitivity across different models remains an open question. This article aims to address the above issue by using three different models, focusing on characteristic structure of simulated precipitation, particularly precipitation extremes.

2. Data and method

2.1. Model and observed data

The daily data from three AGCMs, GFDL-HiRAM, MRI-AGCM and MetUM, each with two resolution configurations for the period 1998–2008 are used in this study. Table 1 shows the details of the models and experiments. The model data of GFDL-HiRAM and MRI-AGCM were obtained from the Coupled Model Intercomparison Project phase 5 (CMIP5, Taylor *et al.*, 2012) data archive, which is operated by the Program for Climate Model Diagnosis and Intercomparison (PCMDI). The simulations of MetUM are from the UPSCALE (UK on PRACE: weather-resolving Simulations of Climate for globAL Environmental risk) project (Mizielinski *et al.*, 2014). The observed precipitation used in this study is the Tropical Rainfall Measuring Mission (TRMM) 3B42 with the resolution 0.25° × 0.25° for 1998–2008 (Huffman *et al.*, 2007). All model data and TRMM are interpolated to the resolution of MetUM-N216 (approximate 0.83° longitude × 0.55° latitude) using distance weighted interpolation method in order to facilitate the comparisons.

2.2. Metrics of evaluation

We use the probability distribution of daily precipitation using histograms in terms of frequency and amount as functions of intensity bins to evaluate model simulations. A precipitation event is defined as one day with daily precipitation ≥ 1 mm day^{-1}. The days with precipitation <1 mm day^{-1} are considered as dry days. For a given grid, precipitation frequency (percentile of precipitation amount) in each intensity bin is the ratio of the number of the days (accumulated precipitation amount) whose precipitation rate is within the corresponding intensity interval to the number of all days with precipitation >1 mm day^{-1} (total rainfall amount) during 1998–2008. Since the frequency and amount percentile greatly differs among individual bins, the ratio of simulated bias of low resolution models (difference between high and low resolution models) to that of each bin in TRMM is used to measure the relative bias (improvement of high resolution models).

Two other metrics are selected to represent extreme dry and very wet conditions. The former index is the maximum length of consecutive dry days with precipitation <1 mm day^{-1} (CDD). Given the percentile thresholds differs among models and TRMM, the later index used to stand for very wet condition is the fraction of R95P, which is defined as the total precipitation due to very wet days with precipitation amounts exceeding the 95th percentile on wet days (daily precipitation ≥ 1 mm day^{-1}) for each grid in the base period 1998–2008.

3. Result

3.1. Simulation of precipitation structure

The distributions of daily precipitation frequency and percentile of amount as a function of daily mean

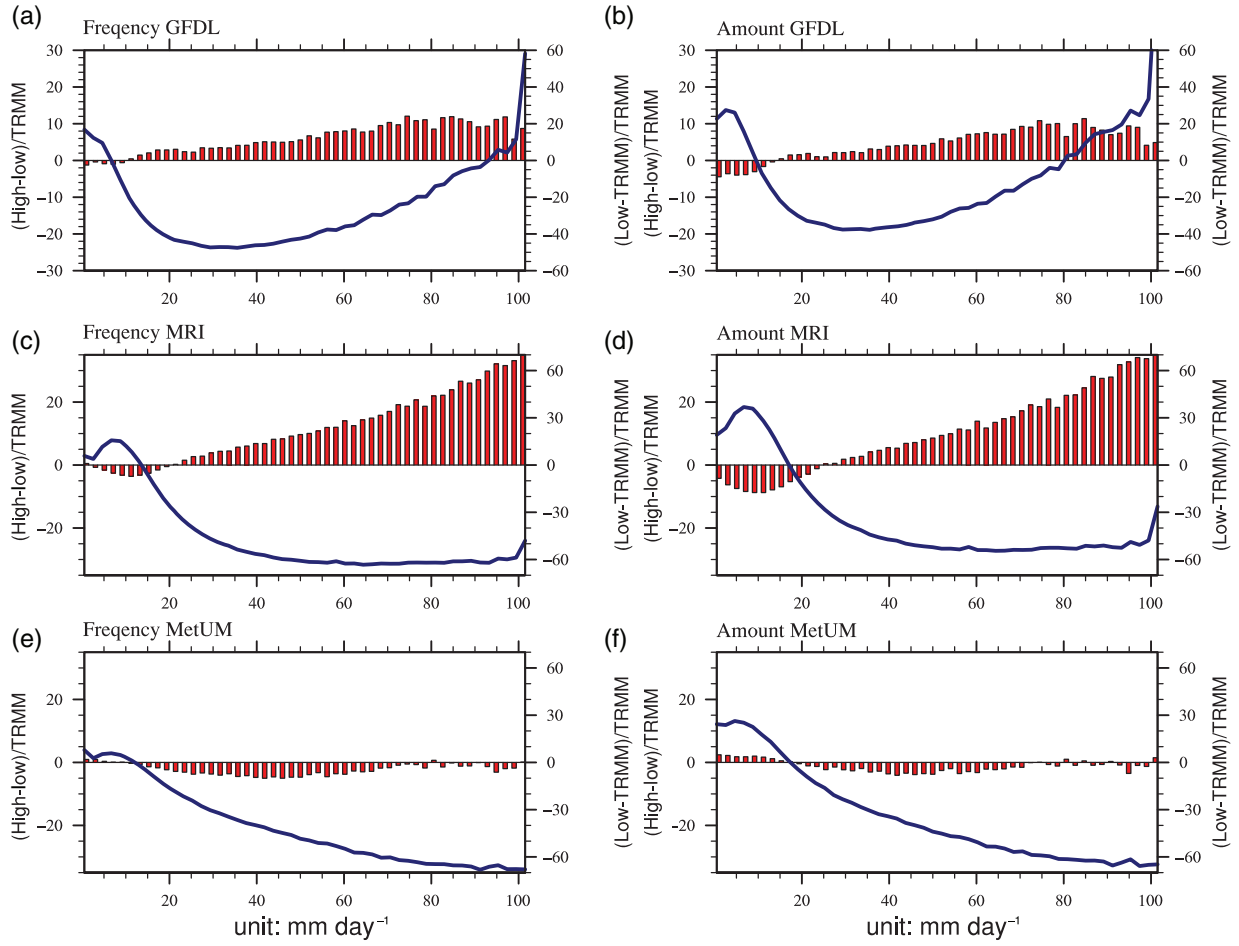

Figure 1. Percentile histograms (bin size 2 mm day^{-1}) of frequency (a, c, e) and amount (b, d, f) differences in daily precipitation characteristics between low resolution models and TRMM (blue line, right axis, unit: %) and between high and low resolutions of the same model (red bar, left axis, unit: %) for a 11-year period 1998–2008 covering the globe between 50°S and 50°N. The unit of the *x*-axis is mm day^{-1}. Both differences are shown as percentages relative to the baseline.

precipitation intensity from 1 to 100 mm day^{-1} averaged over (50°S–50°N, 0°–360°E) derived from TRMM both show a maximum percentile around the 1–3 mm day^{-1} (37% for frequency and 8.3% for amount percentile), with decreasing percentile towards high daily precipitation rates (Figure A1). All three models with low resolution well reproduce these observed precipitation characteristics (lines in Figure A1). However, the ratio of difference between low resolution mode and TRMM relative to that of TRMM in each bin (blue lines in Figure 1) shows that all three models tend to overestimate both the frequency and amount percentile of light rainfall amounts ($1 \sim 11$ mm day^{-1}), but two models underestimate moderate to heavy rainfall totals (>20 mm day^{-1}) (blue lines in Figure 1) and the third model GFDL-HiRAM-C180 shows higher frequency in the bin >90 mm day^{-1} and amount percentile in the bins >80 mm day^{-1} (blue lines in Figures 1(a) and (b)) than TRMM. The maximum overestimation of precipitation frequency (amount) within bins $1 \sim 11$ mm day^{-1} is seen from GFDL_HiRAM-C180 (MRI-AGCM-2H), which greater than TRMM by 17% (37%) in the intensity $1 \sim 3$ mm day^{-1} ($7 \sim 9$ mm day^{-1}), while the maximum underestimation within the bins >11 mm day^{-1} is shown in MRI-AGCM-2H and MetUM-N216 with the bias less than TRMM by 60% when precipitation intensity >61 mm day^{-1}. The separating lines between positive and negative biases for simulating frequency (amount percentile) are 8 mm day^{-1} (10 mm day^{-1}), 16 mm day^{-1} (16 mm day^{-1}) and 10 mm day^{-1} (18 mm day^{-1}) for GFDL-HiRAM-C180, MRI-AGCM-2H and MetUM-N216, respectively.

The above-mentioned simulation biases are reduced in higher resolution models of GFDL-HiRAM and MRI-AGCM, through reducing the frequency and amount percentile of low daily precipitation amounts but increasing the medium to heavy rainfall amounts (red bars in Figure 1). In comparison, the improvement of MRI-AGCM-2S is the biggest among the three models, and that in MetUM is not obvious. The accumulated frequency (amount percentile) simulated by MRI-AGCM-2H within the bins 1–11 mm day^{-1} is more than TRMM by 10% (26%), but less than TRMM by 51% (41%) for the bins >11 mm day^{-1}, whereas simulation by MRI-AGCM-2S with bins 1–11 m day^{-1} is only more than TRMM by 9% (20%) and only less than TRMM by 38% (28%) for the bins

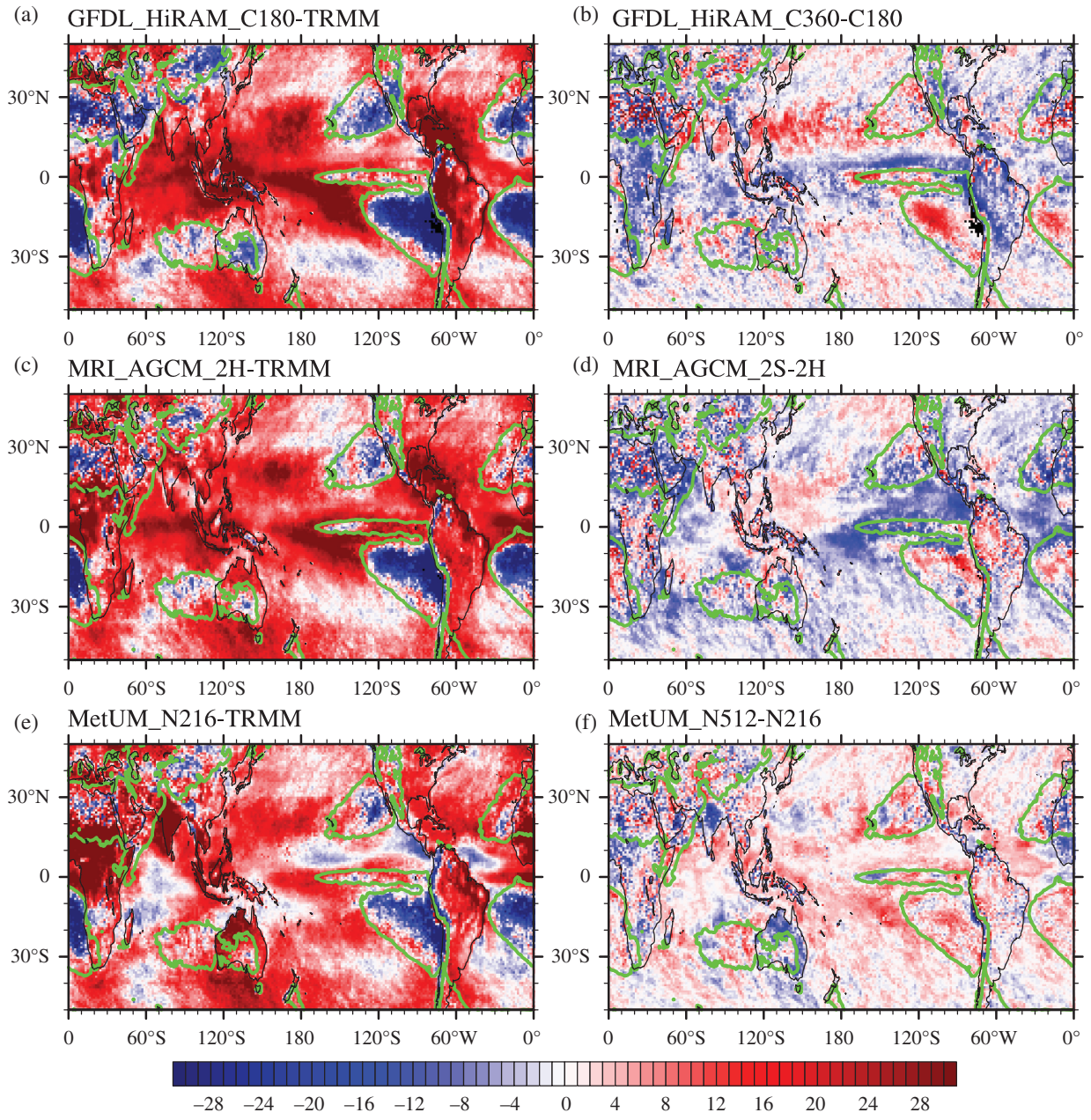

Figure 2. Spatial distributions of difference between low resolution models and TRMM (unit: %, a, c, e) and between high and low resolutions of the same model (unit: %, b, d, f) in simulating amount percentile of light rainfall (bin 1–11 mm day^{-1}). Green lines show the climatological 1 mm day^{-1} contours derived from TRMM.

>11 mm day. The improvement in MetUM-N512 is not obvious relative to the other two AGCMs. Notice that GFDL-HiRAM-C180 tends to overestimate the heavy rainfall amounts with intensity >80 mm day^{-1}. This bias gets more severe as model resolution is increased.

To determine which regions contribute to the global mean bias, the geographical pattern of the frequency and amount percentile are examined. Figure 2 presents the spatial patterns for total amount percentile accounted by light rainfall amounts in TRMM, the bias of low resolution models and the difference between high and low resolution models. The improvements in simulating frequency and amount percentile show similar patterns when increasing the resolution. Thus, only the geophysical distribution of amount percentile is shown. In the observations, light rainfall amounts accounting for 50% of the total rainfall mainly locate in the global desert regions, such as North Africa, central Asia, Southeast Pacific Ocean and South Atlantic Ocean, consistent with the dry areas defined by regions with local summer precipitation <1 mm day^{-1} (Wang *et al.*, 2012) (green lines in Figure 2). All models capture well the features of light rainfall amounts (Figure A2). The low resolution models of the three AGCMs, GFDL-HiRAM-C180, MRI-AGCM-2H and MetUM-N216, overestimate the light rainfall amount percentile over most parts of the world but the desert regions (left panel in Figure 2). Inspection on the difference between high and low resolution finds that the bias over the desert regions are generally reduced

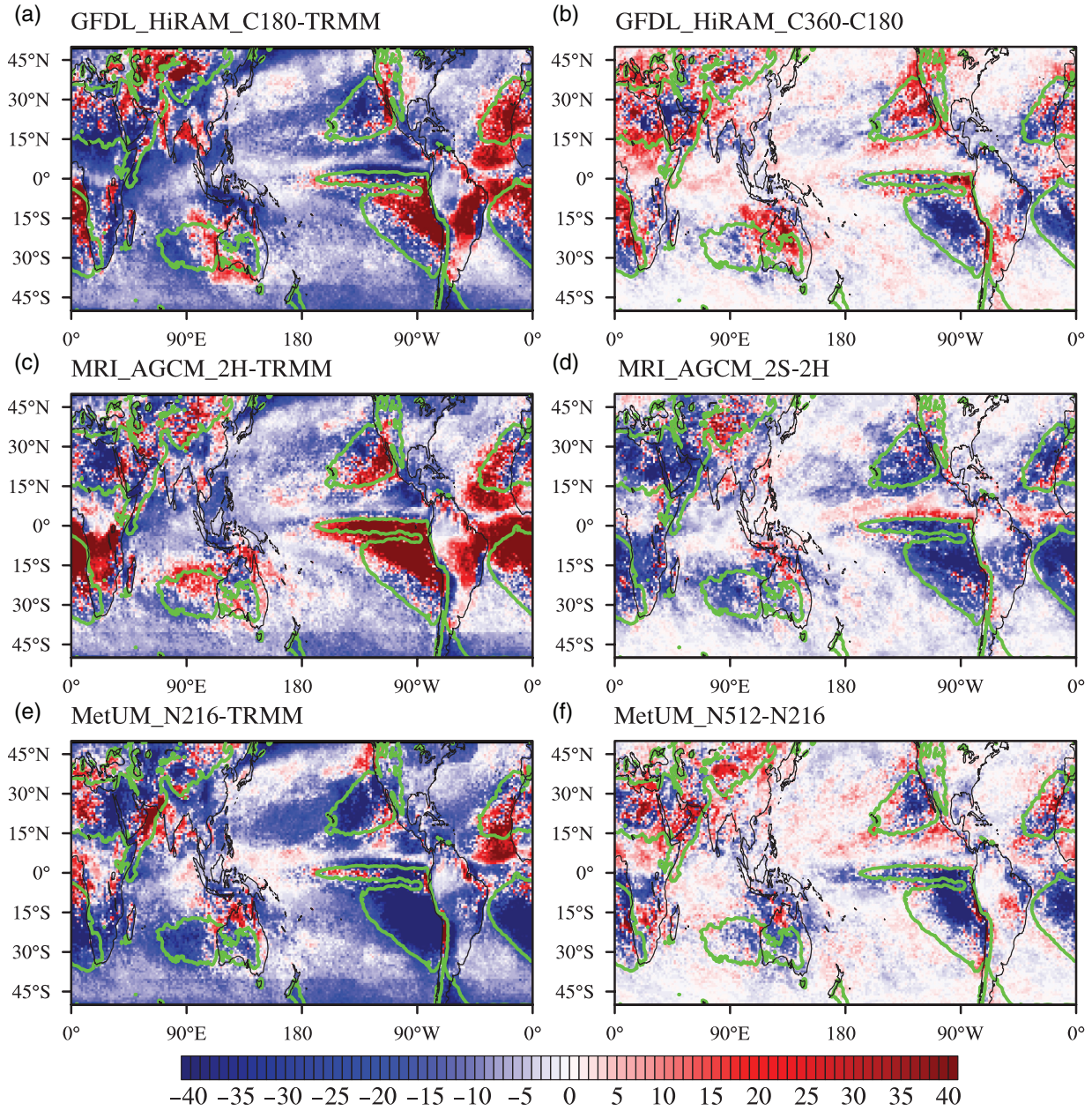

Figure 3. Same as Figure 2, but for CDD (days per year).

in the three high resolution models (right panel in Figure 2). The bias is reduced in GFDL-HiRAM-C360 and MRI-AGCM-2S in the tropical southern and eastern Pacific but increases in the tropical northern and western, while it changes little in MetUM-N512. The largest discrepancy across the three models is evident over the ocean. For instance, in MetUM-N216 both the overestimation and underestimation bias on light rainfall amount percentile over the South Pacific Ocean and Atlantic Ocean becomes larger in high resolution configuration, while these biases are reduced in the other two AGCMs. The overall higher percentile of light rainfall over ocean in MetUM-N512 induces unique response of MetUM to higher resolution as shown in Figure 1. We also notice that high resolution configuration of all models increases the fraction of light rainfall amounts over Northwest Pacific Ocean (0°–20°N, 120°–180°E), leading to a poorer performance than their low resolution models.

Besides the distribution for percentile of light rainfall amount, the distributions for percentile account by medium to heavy rainfall ($\geq$11 mm day^{-1}) amounts are also assessed. The corresponding patterns are opposite to light rainfall (Figure A3), because the total percentile of light rainfall and medium to heavy rainfall is 100%. The over underestimation of precipitation percentile with intensity >11 mm day^{-1} over globe is increased in the high resolution models of GFDL-HiRAM and MRI-AGCM-2S, while little in MetUM-N512. The above discussion shows that higher model resolution produces added value in simulating precipitation structure by reducing the percentage of light rainfall amounts and increasing percentage of medium to heavy rainfall amounts.

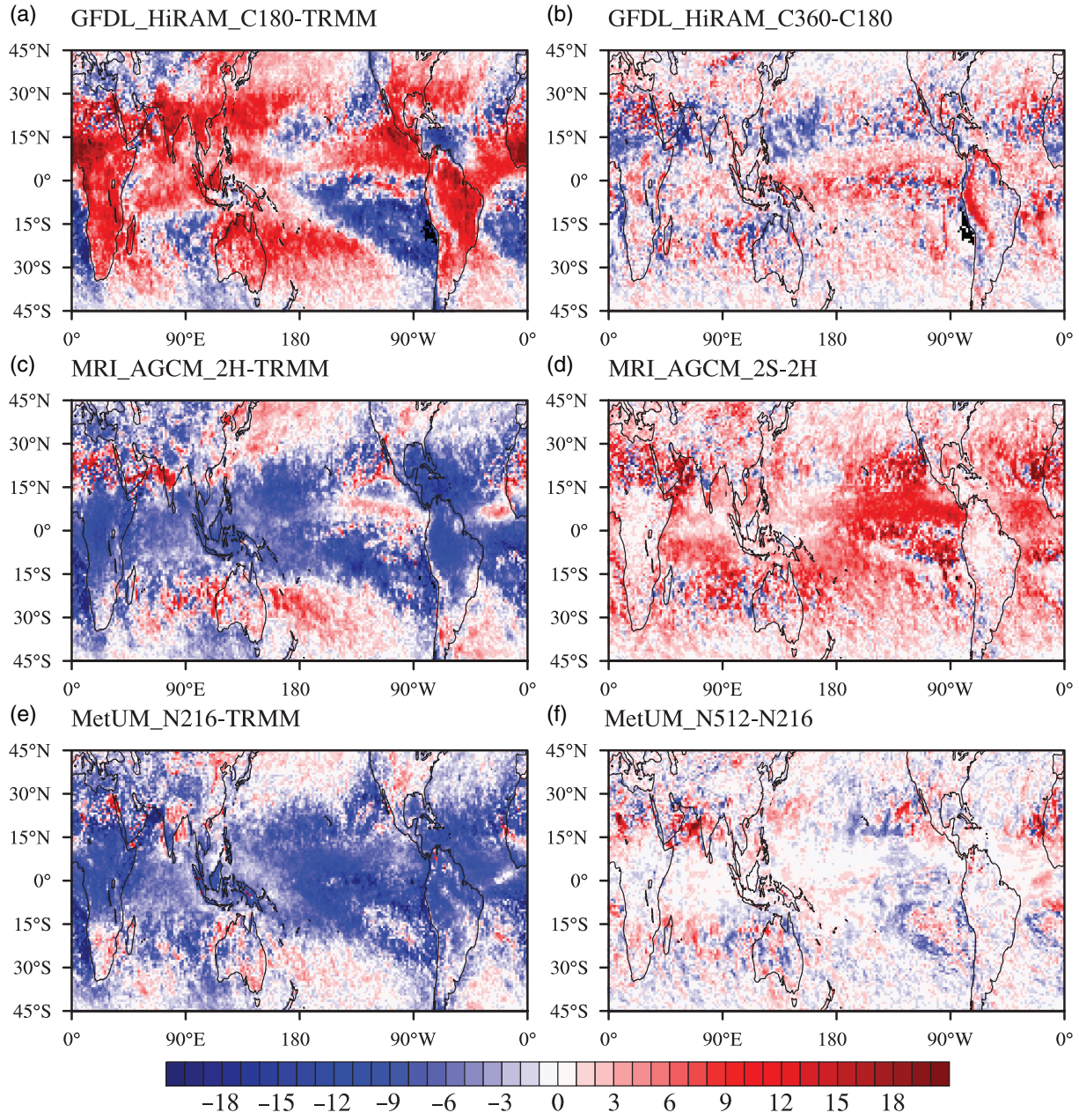

Figure 4. Same as Figure 2, but for the distributions for the fraction of total precipitation due to very wet days with precipitation amounts exceeding the 95th percentile on wet days (daily precipitation $\geq$ 1 mm day^{-1}) in the base period 1998–2008 (R95P).

3.2. Simulation of extreme precipitation

Same as Figure 2, the biases in low resolution models and improvement of high resolution in simulating CDD are shown in Figure 3. The observed CDD centres are seen over the dry regions, with a maximum over the Southern Hemispheric ocean desert regions and Sahara desert reaching 300-day per year and minimum over the Intertropical Convergence Zone (ITCZ) falling below 10-day per year (Figure A4 and regions denoted by green lines in Figure 3). The three low resolution AGCMs exhibit different simulation biases. In GFDL-HiRAM-C180 and MRI-AGCM-2H, the CDD in oceanic dry regions is overestimated, but that in tropical Indian Ocean and equatorial eastern Pacific Ocean is underestimated, with the largest positive bias (>50 days) over the south-eastern Pacific and South Atlantic oceans and largest negative bias (<−50 days) over the tropical Indian Ocean. In contrast, an overall negative bias of the globe is seen from MetUM-N216, except tropical part of the oceanic dry regions and North Indian Ocean (10°–25°N, 50°–100°E) (Figure 3(e)).

Although the above-mentioned biases still exist in the high resolution models, the biases are systematically reduced when increasing resolution (Figures 3(b), (d) and (f)). Comparing with low resolution models, a reduction of CDD over oceanic desert regions is seen from all three high resolution AGCMs, which is consistent with the increase of light rainfall contribution there (Figures 2(b), (d) and (f)). The maximum reduction of CDD when increasing resolution is seen over

south-eastern Pacific desert region exceeding 80 days, which reaches the magnitude of observed standard deviation (Figure A5). In addition, the CDD over land in both GFDL-HiRAM-C360 and MetUM-N512 (MRI-AGCM-2S) is increased (reduced) relative to their low resolution configurations. Smaller root mean square errors (RMSE) against TRMM are shown in GFDL-HiRAM-C180 and MRI-AGCM-2S (29.6 and 35.7 days) relative to their low resolution configurations (37.7 and 45.2 days), while an even larger RMSE in MetUM-N512. However, the negative biases over the dry regions of North-eastern Pacific become larger when increasing resolution of GFDL-HiRAM and MetUM models.

The spatial distributions for fraction of R95P, simulation biases in low resolution models and the differences between high and low resolution models are shown in Figure 4. The maximum fraction of R95P in TRMM is centred in the mid-latitude in both hemisphere along the belts of 10°–30°N and 10°–30°S (Figure A6 in the Appendix), mainly located in global monsoon regions. The fraction of R95P over the ITCZ is relatively small. It indicates that about one-third rainfall falling in the global monsoon region occurs in extreme rainfall days, while the contribution of extreme rainfall over ITCZ to total rainfall is relatively small although its total rainfall is large. The three low resolution models partly capture the observed distribution, and the highest pattern correlation coefficient against TRMM is 0.43 in MRI-AGCM-2H. The simulation bias of low resolution models differs across the three AGCMs. For instance, an overall overestimation of extreme precipitation is shown in GFDL-HiRAM-C180, but underestimation in both MRI-AGCM-2H and MetUM-N216 (Figures 4(a), (c) and (e)).The maximum fraction of R95P in GFDL-HiRAM-180 over the global monsoon regions reaches 60%, which is up to twice of the TRMM, while the area with fraction <15% over Southeast Pacific and South Atlantic Ocean is much smaller than TRMM (Figures 4(b) and (e)). An overall underestimation of fraction of R95P is simulated by both MRI-AGCM-2H and MetUM-N216 (Figures 4(c) and (e)). These simulation biases are consistent with their bin biases as shown in Figure 1.

The impacts of improving model resolution differ greatly across the three AGCMs. In general, the overall positive bias in GFDL-HiRAM-C180 and negative bias in MRI-AGCM-2H are reduced in their high resolution models. Comparing with GFDL-HiRAM-C180, the fraction of R95P is reduced by 20% in maximum over the Africa-India-Northwestern Pacific monsoon region in GFDL-HiRAM-C360 and increased by 20% in maximum over the Southeast Pacific, which reduces the simulation bias of its low resolution model. High resolution makes an overall increase of the fraction of R95P in MRI-AGCM-2S with the maximum improvement over the tropical Pacific and Atlantic Ocean, while little improvement in MetUM-N512 (Figures 4(b), (d) and (f)). Although an improvement of simulation skill in fraction of R95P is found in high resolution models, both the simulation bias of low resolution models and the responses to high resolution greatly differ across the three models, indicating that the simulation of extreme wet precipitation greatly depend on the model dynamic processes and parameterization schemes.

4. Summary

Using the simulations from three AGCMs, GFDL-HiRAM, MRI-AGCM and MetUM, each with two resolution configurations, this article investigated the added values of high resolution in simulating the global precipitation frequency and amount percentile as functions of daily mean intensity bins and the impact of resolution on extreme precipitation. Consistency and discrepancy responses across the three AGCMs to increasing model resolution were found in this study, which were summarized as following:

1. A common simulation bias across the three models was an overestimation of light rainfall (intensity 1–11 mm day^{-1}) frequency and amount and underestimation of medium rainfall (intensity 20–80 mm day^{-1}). High resolution helped to reduce both global mean frequency and amount percentile of light rainfall and increase those of medium amounts in GFDL-HiRAM-C180 and MRI-AGCM-2H, while the precipitation structure in the MetUM high resolution model changed slightly. The overestimation of frequency and amount percentile of light rainfall over most parts of the globe and the underestimation over dry regions became smaller in high resolution models of GFDL-HiRAM and MRI-AGCM.
2. A consistent response to high resolution across the three AGCMs was seen from the light rainfall frequency/amount and CDD over the desert regions, particularly over the ocean desert regions. Comparing with the low resolution models, an increase of light rainfall contribution over the desert regions was shown in all three high resolution models. Consequently, the CDD over the oceanic dry regions was shortened in the high resolution models. It suppressed the overestimation of CDD over ocean desert regions and makes a better performance in high resolution configuration of GFDL-HiRAM and MRI-AGCM, but worse in MetUM-N512.
3. With increasing resolution, a better simulation of fraction of R95P was found over most part in MRI-AGCM-2S and the African-Indian-Northwestern Pacific monsoon region in GFDL-HiRAM-C360, but the simulation skill of the third model MetUM changed little. Unlike the simulation of light rainfall and CDD, consistency among the three models was small in simulating extreme wet precipitation contribution since both the simulation biases in the low resolution models and the responses to high resolution differ greatly across the three models. It might indicate that the simulation on extreme wet precipitation depends much on model dynamical and physical processes.

Although improvements of light rainfall can arise from increased horizontal resolution due to the consistent response of the three models to high resolution, large model discrepancies exist across the three models, most of which can be found over tropical oceanic strong convection regions. For example, comparing with their corresponding low resolution models, the percentile accounted by light rainfall over the tropical southern Pacific becomes larger in MetUM-N512 but smaller in the other two models. The impacts of higher model resolution on the simulation of fraction of R95P differ greatly across the three AGCMs. These discrepancies can be partially ascribed to the different reactions of some dynamical and physical processes to the resolution. Therefore, key dynamic processes and parameterization schemes are also crucial aspects for better and more reasonable simulation in high resolution models.

Acknowledgements

We thank Gill Martin for her valuable comments on this work. This work was jointly supported by the National Natural Science Foundation of China under grant nos. 41305072, 41330423 and 41675076, and R&D Special Fund for Public Welfare Industry (meteorology) (GYHY201506012). Met Office staff are supported by the UK-China Research & Innovation Partnership Fund through the Met Office Climate Science for Service Partnership (CSSP) China as part of the Newton Fund.

Appendix

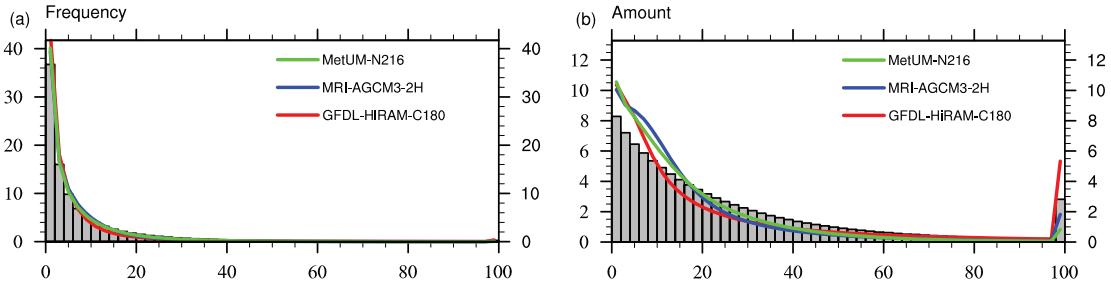

Figure A1. Percentile histograms (bin size 2 mm day^{-1}) of frequency (a) and amount percentile (b) (unit: %) in daily precipitation derived from TRMM and the low resolution models for 1998–2008 covering the globe between 50°S and 50°N.

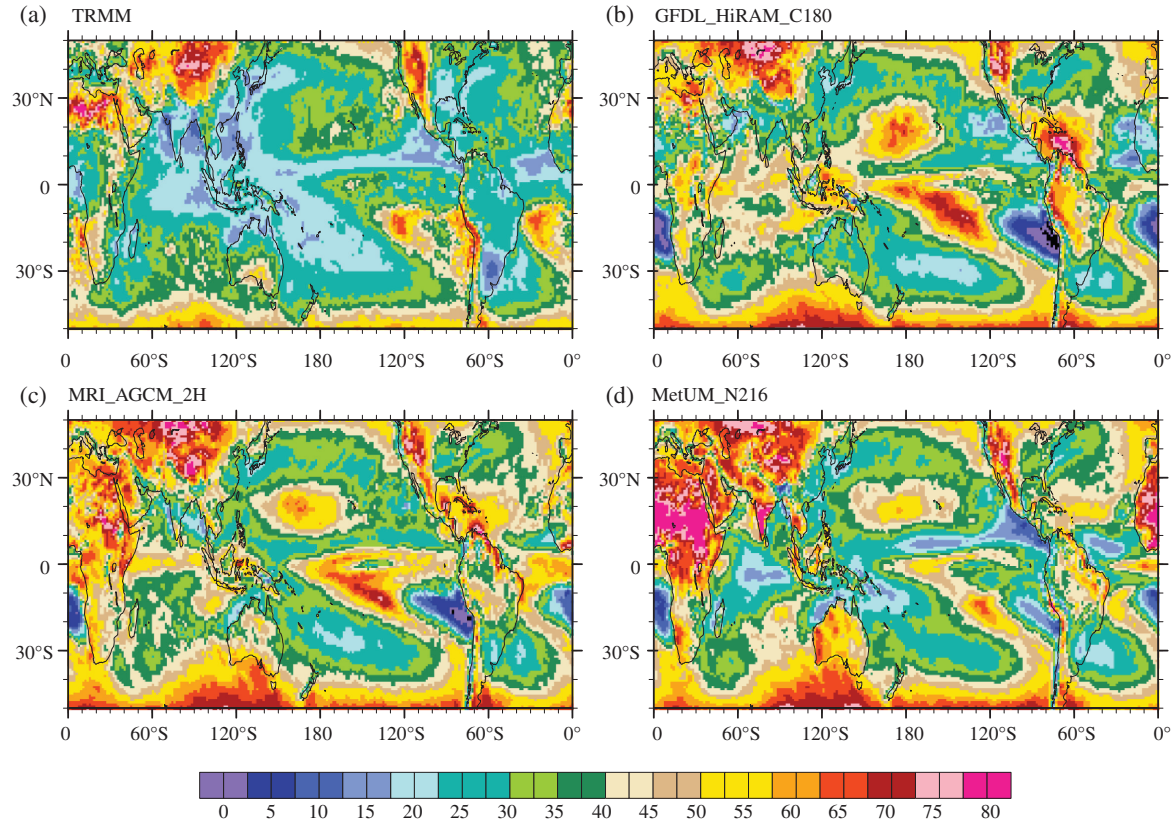

Figure A2. Spatial distribution of amount percentile (unit: %) of light rainfall (bin 1–11 mm day^{-1}) from (a) TRMM, (b) GFDL-HiRAM-C180, (c) MRI-AGCM-2H and (d) MetUM-N216.

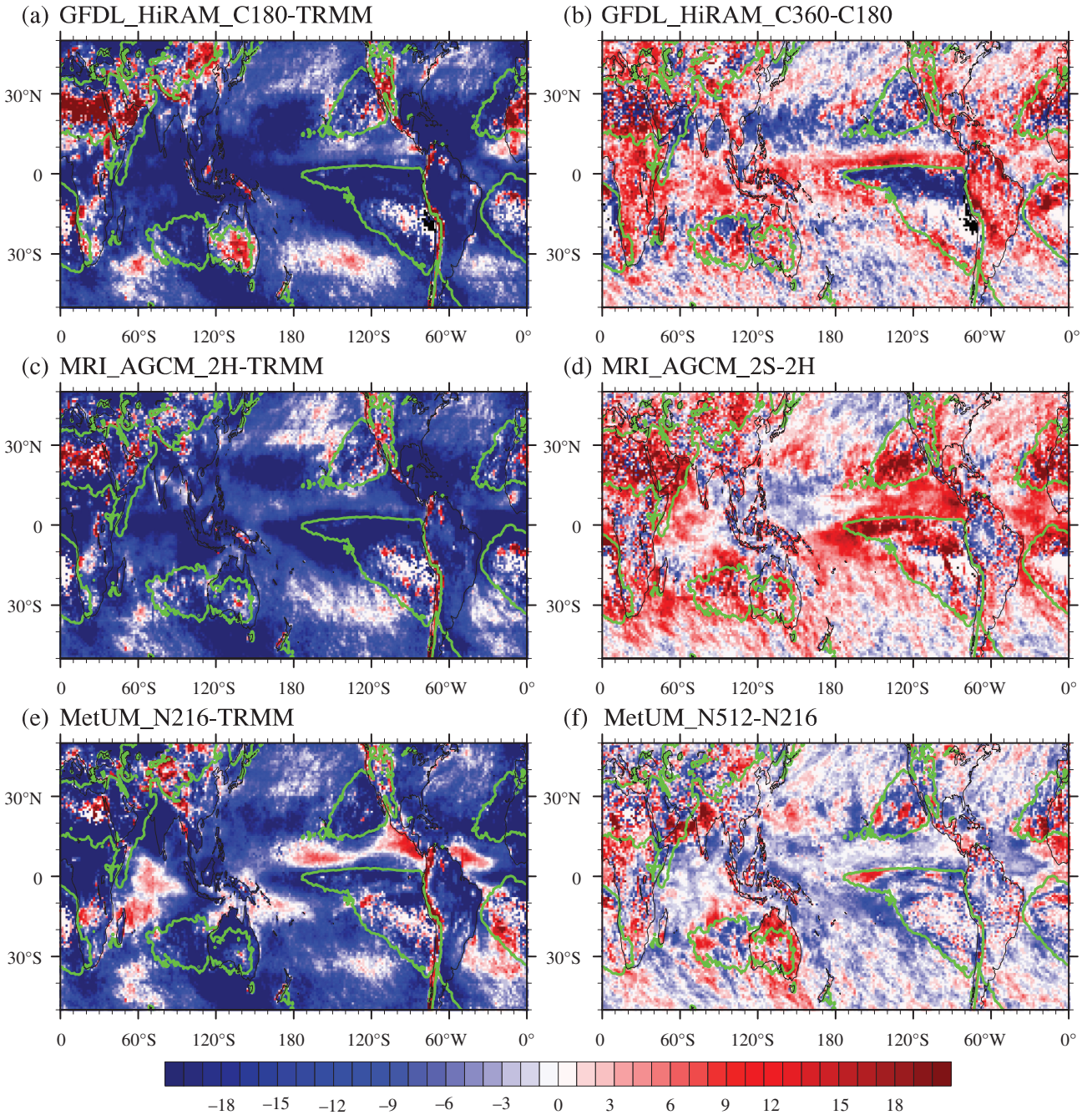

Figure A3. Spatial distribution of difference between low resolution models and TRMM (unit: %, a, c, e) and between high and low resolutions models (unit: %, b, d, f) in simulating amount percentile of medium to heavy daily rainfall (bin > 11 mm day^{-1}). Green lines show the climatological 1 mm day^{-1} contours derived from TRMM.

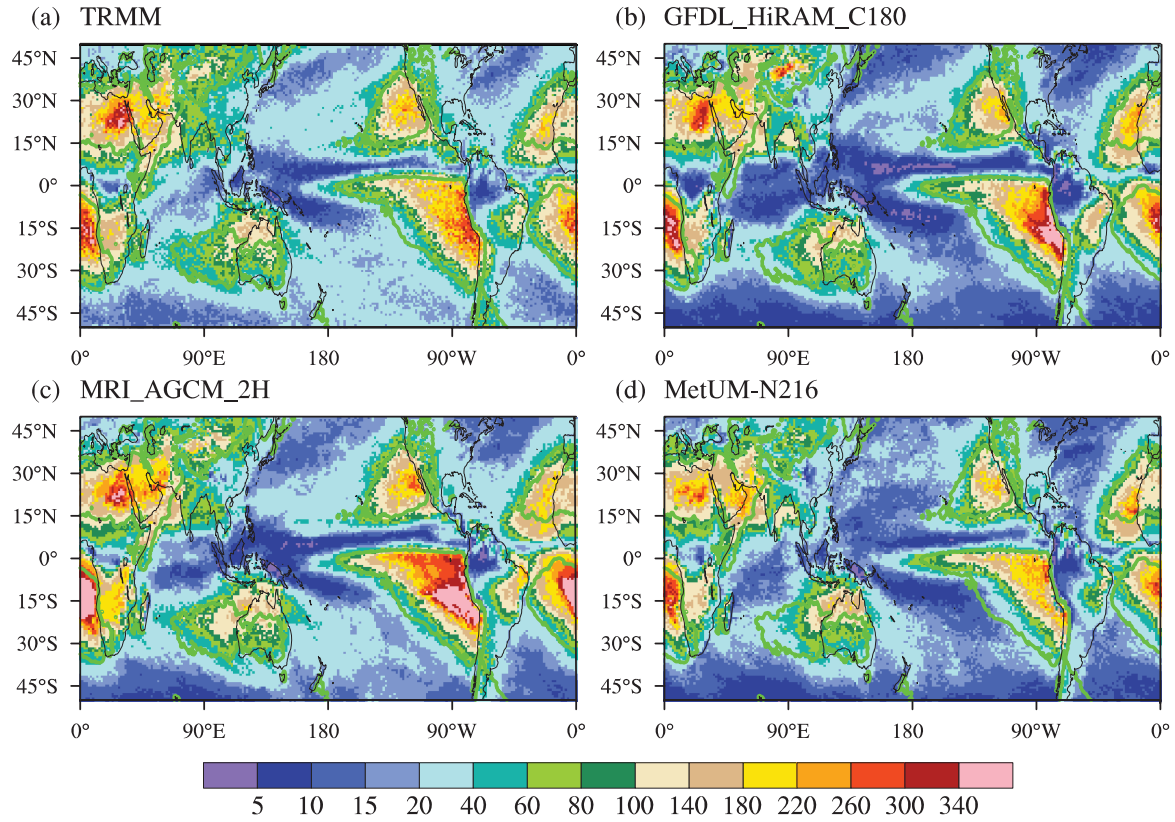

Figure A4. Spatial distribution of climatological CDD (day per year) for 1998–2008 from (a) TRMM, (b) GFDL-HiRAM-C180, (c) MRI-AGCM-2H and (d) MetUM-N216.

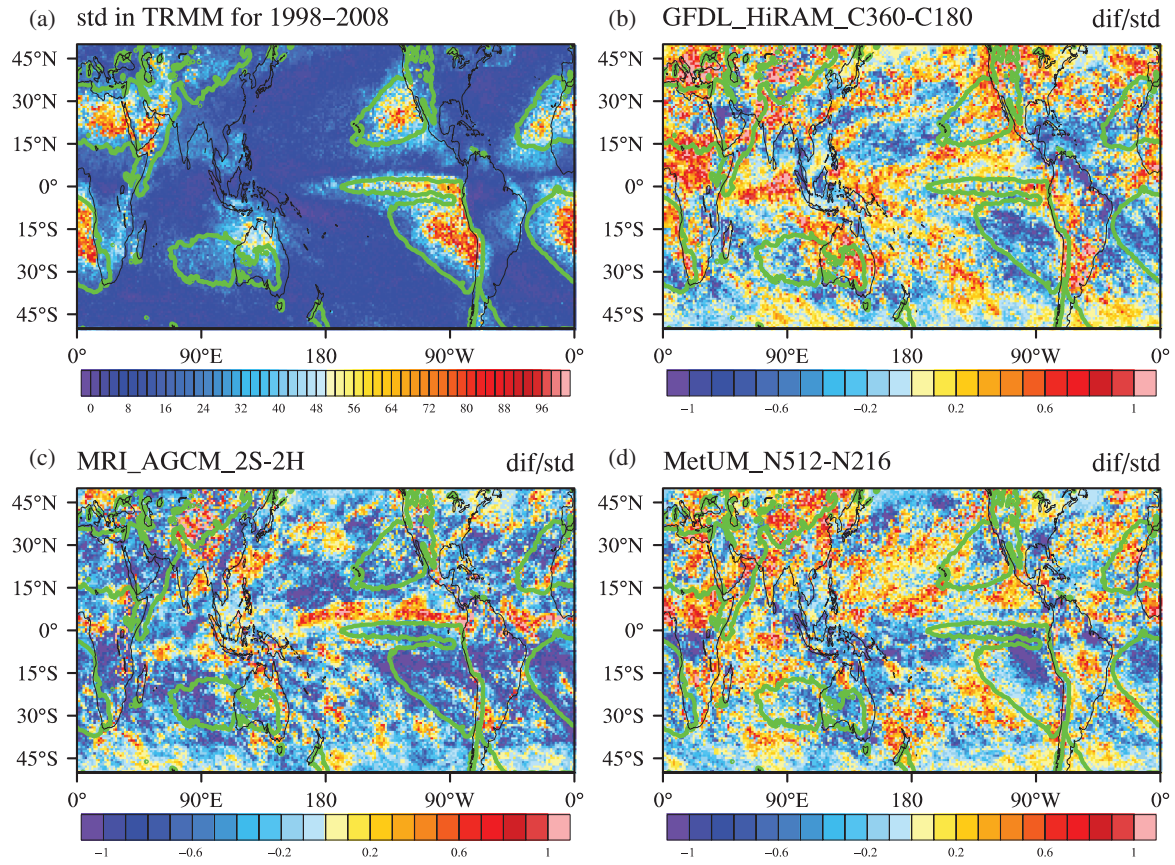

Figure A5. Spatial distribution for (a) standard deviation of CDD (day) during 1998–2008, and (b)–(d) ratio of difference between high and low resolution models to the standard deviation of TRMM.

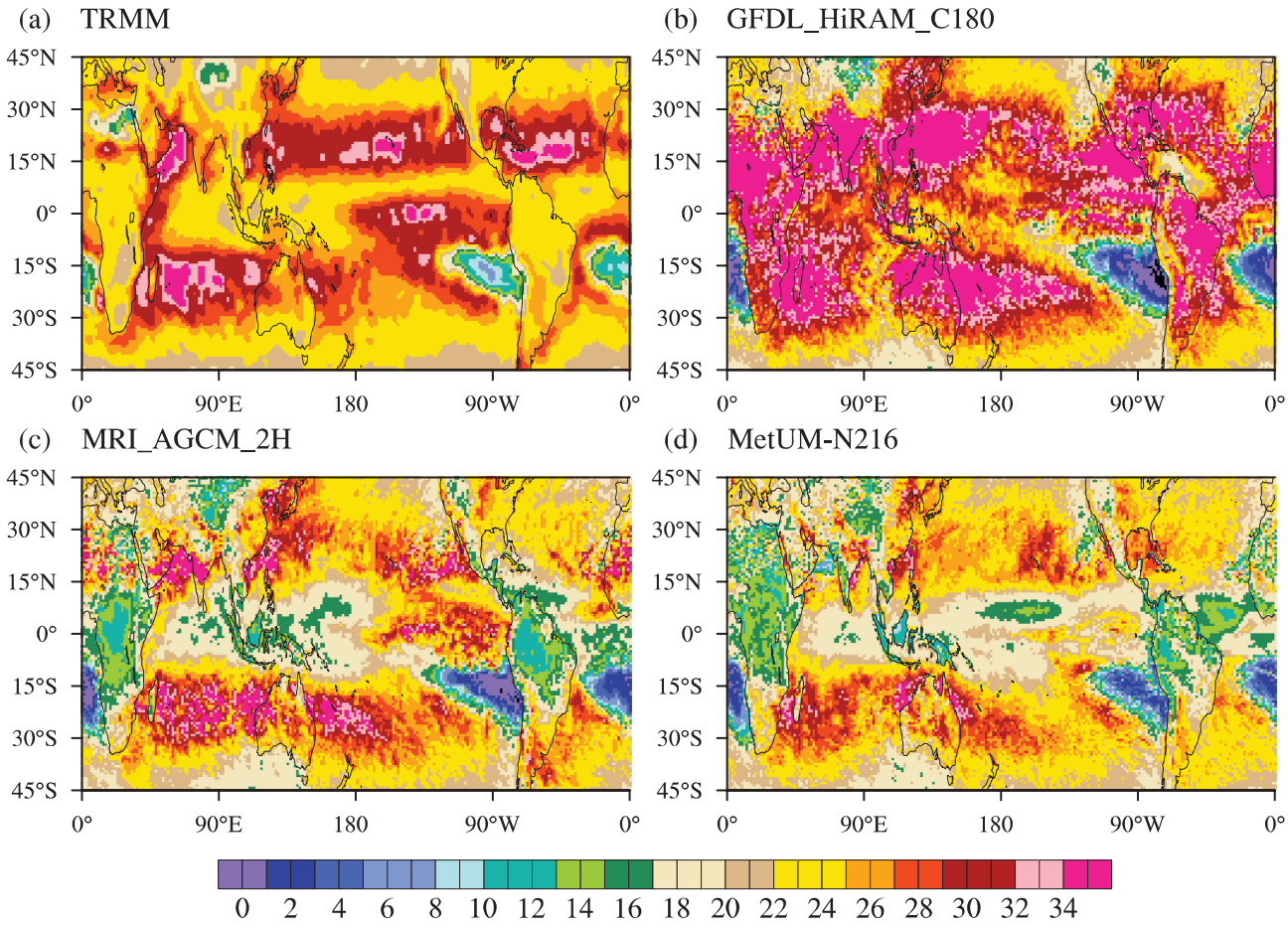

Figure A6. Same as Figure A4, but for the fraction of R95P (%).

References

Dai A. 2006. Precipitation characteristics in eighteen coupled climate models. *Journal of Climate* **19**: 4605–4630, doi: 10.1175/JCLI3884.1.

Delworth TL, Rosati A, Anderson W, Adcroft AJ, Balaji V, Benson R, Dixon K, Griffies SM, Lee HC, Pacanowski RC, Vecchi GA, Wittenberg AT, Zeng F, Zhang R. 2012. Simulated climate and climate change in the GFDL CM2.5 high-resolution coupled climate model. *Journal of Climate* **25**: 2755–2781, doi: 10.1175/JCLI-D-11-00316.1.

Demory M-E, Vidale PL, Roberts MJ, Berrisford P, Strachan J, Schiemann R, Mizielinski M. 2014. The role of horizontal resolution in simulating drivers of the global hydrological cycle. *Climate Dynamics* **42**(7): 2201–2225, doi: 10.1007/s00382-013-1924-4.

Donlon CJ, Martin M, Stark J, Roberts-Jones J, Fiedler E, Wimmer W. 2012. The Operational Sea Surface Temperature and Sea Ice Analysis (OSTIA) system. *Remote Sensing of Environment* **116**: 140–158, doi: 10.1016/j.rse.2010.10.017.

Huffman GJ, Bolvin DT, Nelkin EJ, Wolff DB, Adler RF, Gu G, Hong Y, Bowman KP, Stocker EF. 2007. The TRMM multisatellite precipitation analysis (TMPA): quasi-global, multiyear, combined-sensor precipitation estimates at fine scales. *Journal of Hydrometeorology* **8**(1): 38–55.

Johnson T, Levin R, Turner A, Martin G, Woolnough SW, Schiemann R, Mizielinski SM, Roberts MJ, Vidale PL, Demory M, Strachan J. 2015. The resolution sensitivity of the South Asian monsoon and Indo-Pacific in a global 0.35° AGCM. *Climate Dynamics* **46**(3): 807–831, doi: 10.1007/s00382-015-2614-1.

Jung T, Gulev SK, Rudeva I, Soloviov V. 2006. Sensitivity of extratropical cyclone characteristics to horizontal resolution in the ECMWF model. *Quarterly Journal of the Royal Meteorological Society* **132**: 1839–1857, doi: 10.1256/qj.05.212.

Jung T, Miller MJ, Palmer TN, Towers P, Wedi N, Achuthavarier D, Adams JM, Altshuler EL, Cash BA, III JLK, Marx L, Stan C, Hodges KI. 2012. High-resolution global climate simulations with the ECMWF model in project Athena: experimental design, model climate, and seasonal forecast skill. *Journal of Climate* **25**: 3155–3172, doi: 10.1175/JCLI-D-11-00265.1.

Kinter JL III, Cash B, Achuthavarier D, Adams J, Altshuler E, Dirmeyer P, Doty B, Huang B, Jin EK, Marx L, Manganello J, Stan C, Wakefield T, Palmer T, Hamrud M, Jung T, Miller M, Towers P, Wedi N, Satoh M, Tomita H, Kodama C, Nasuno T, Oouchi K, Yamada Y, Taniguchi H, Andrews P, Baer T, Ezell M, Halloy C, John D, Loftis B, Mohr R, Wong K. 2013. Revolutionizing climate modeling with project Athena: a multi-institutional, international collaboration. *Bulletin of the American Meteorological Society* **94**: 231–245, doi: 10.1175/BAMS-D-11-00043.1.

Kitoh A, Kusunoki S. 2008. East Asian summer monsoon simulation by a 20-km mesh AGCM. *Climate Dynamics* **31**: 389–401, doi: 10.1007/s00382-007-0285-2.

Kusunoki S, Arakawa O. 2012. Changes in the precipitaiton intensity of the East Asian summer monsoon projected by CMIP3 models. *Climate Dynamics* **38**(9): 2055–2072.

Li J, Yu R, Yuan W, Chen H, Sun W, Zhang Y. 2015. Precipitation over East Asia simulated by NCAR CAM5 at different horizontal resolutions. *Journal of Advances in Modeling Earth Systems* **7**(2): 774–790, doi: 10.1002/2014MS000414.

Manganello JV, Hodges KI, III JLK, Cash BA, Marx L, Jung T, Achuthavarier D, Adams JM, Altshuler EL, Huang B, Jin EK, Stan C, Towers P, Wedi N. 2012. Tropical cyclone climatology in a 10-km global atmospheric GCM: toward weather-resolving climate modeling. *Journal of Climate* **25**: 3867–3893, doi: 10.1175/JCLI-D-11-00346.1.

Marti O, Braconnot P, Dufresne JL, Bellier J, Benshila R, Bony S, Brockmann P, Cadule P, Caubel A, Codron F, de Noblet N, Denvil S,

Fairhead L, Fichefet T, Foujols MA, Friedlingstein P, Goosse H, Grandpeix JY, Guilyardi E, Hourdin F, Idelkadi A, Kageyama M, Krinner G, Levy C, Madec G, Mignot J, Musat I, Swingedouw D, Talandier C. 2010. Key features of the IPSL ocean atmosphere model and its sensitivity to atmospheric resolution. *Climate Dynamics* **34**: 1–26, doi: 10.1007/s00382-009-0640-6.

Mizielinski MS, Roberts MJ, Vidale PL, Schiemann R, Demory M-E, Strachan J, Edwards T, Stephens A, Lawrence BN, Pritchard M, Chiu P, Iwi A, Churchill J, Del Cano Novales C, Kettleborough J, Roseblade W, Selwood P, Foster M, Glover M, Malcolm A. 2014. High resolution global climate modelling; the UPSCALE project, a large simulation campaign. *Geoscientific Model Development* **7**: 563–591.

Mizuta R, Yoshimura H, Murakami H, Matsueda M, Endo H, Ose T, Kamiguchi K, Hosaka M, Sugi M, Yukimoto S, Kusunoki S, Kitoh A. 2012. Climate simulations using MRI-AGCM3.2 with 20-km grid. *Journal of the Meteorological Society of Japan* **90A**: 233–258, doi: 10.2151/jmsj.2012-A12.

Palmer T. 2014. Build high-resolution global climate models. *Nature* **515**: 338–339.

Rayner NA, Parker DE, Horton EB, Folland CK, Alexander LV, Rowell DP, Kent EC, Kaplan A. 2003. Global analyses of sea surface temperature, sea ice, and night marine air temperature since the late nineteenth century. *Journal of Geophysical Research* **108**(D14): 4407, doi: 10.1029/2002JD002670.

Roberts MJ, Clayton A, Demory ME, Donners J, Vidale PL, Norton W, Shaffrey L, Stevens DP, Stevens I, Wood RA, Slingo J. 2009. Impact of resolution on the tropical Pacific circulation in a matrix of coupled models. *Journal of Climate* **22**(10): 2541–2556, doi: 10.1175/2008JCLI2537.1.

Shaffrey LC, Stevens I, Norton WA, Roberts MJ, Vidale PL, Harle JD, Jrrar A, Stevens DP, Woodage MJ, Demory ME, Donners J, Clark DB, Clayton A, Cole JW, Wilson SS, Connolley WM, Davies TM, Iwi AM, Johns TC, King JC, New AL, Slingo JM, Slingo A, Steenman-Clark L, Martin GM. 2009. UK HiGEM: the new UK high-resolution global environment model – model description and basic evaluation. *Journal of Climate* **22**(8): 1861–1896, doi: 10.1175/2008JCLI2508.1.

Taylor KE, Stouffer R, Meehl GA. 2012. An overview of CMIP5 and the experiment design. *Bulletin of the American Meteorological Society* **93**: 485–498.

Tu K, Yan ZW, Zhang XB, Dong WJ. 2009. Simulation of precipitation in monsoon regions of China by CMIP3 models. *Atmospheric and Oceanic Science Letters* **2**: 194–200.

Wang B, Liu J, Kim HJ, Webster PJ, Yim SY. 2012. Recent change of the global monsoon precipitation (1979–2008). *Climate Dynamics* **39**: 1123–1135.

Yu RC, Li J, Zhang Y, Chen HM. 2015. Improvement of rainfall simulation on the steep edge of the Tibetan Plateau by using a finite-difference transport scheme in CAM5. *Climate Dynamics* **45**(9): 2937–2948, doi: 10.1007/s00382-015-2515-3.

Zhao M, Held IM, Lin S-J, Vecchi GA. 2009. Simulations of global hurricane climatology, interannual variability, and response to global warming using a 50-km resolution GCM. *Journal of Climate* **22**: 6653–6678, doi: 10.1175/2009JCLI3049.1.